UMT PRESS

Journal of Sustainability Science and Management
Journal Homepage: https://jssm.umt.edu.my
eISSN: 2672-7226
DOI: http://doi.org/10.46754/jssm.2026.03.012

PREPARATION OF NEW ACTIVATED CARBON FROM INDUSTRIAL WASTES BY CARBONISATION METHOD INCORPORATED KOH ACTIVATION FOR FAST REMOVAL OF OILY POLLUTANTS FROM REFINERY WASTEWATER

TALIB SUBKH* AND RAGHAD ALMILLY

Chemical Engineering Department, Baghdad University, Baghdad, Iraq.

**Corresponding author: talib.subkh1507m@coeng.uobaghdad.edu.iq*

ARTICLE INFO

Article History:
Received: 2 February 2025
Revised: 21 March 2025
Accepted: 27 April 2025
Published: 15 March 2026

Keywords:
Adsorption process, water treatment, oil pollutants, activation agents, optimisation.

ABSTRACT

This work prepared two new Activated Carbon (AC) from Plastic Waste (PW) and Upholstery Waste (UW) by carbonisation method and activation by alkali agent (potassium hydroxide, KOH) to remove oil pollutants from Refinery Wastewater (RWW) through a batch technique and compared between them. The Fourier Transform Infrared (FTIR) spectroscopy, Field Emission Scanning Electron Microscopy (FESEM), Energy Dispersive X-ray (EDX) spectroscopy, X-ray Diffraction (XRD), and Brunauer–Emmett–Teller (BET) were used to characterise the physicochemical characteristics of the AC as received and KOH/AC of two samples (AC1 and AC2) from PW and UW, respectively. The removal effectiveness of oil pollutants was examined in relation to four operational conditions dose (0.2 to 1 gm), pH (3 to 9), agitation speed (100 to 300), and contact duration (30 to 120 minutes). The removal efficiency under various working conditions was studied to assess the surface efficiency of oil removal on prepared activated carbon treated with KOH, whose specific surface areas increased. The largest oil removal efficiency was 94.7% and 90.8% of AC2, and AC1 at 1 gm, 3 pH, 300 rpm, and 120 minutes, respectively, obtained with AC/KOH, which presented a superior adsorption efficiency for oil removal in refinery wastewater.

Introduction

The treatment recognised as adsorption occurs when a gas or liquid solution gathers on an adsorbent surface, producing a molecular film on the adsorbent's surface made up of the molecules being collected (Hassan, 2025). The adsorbent molecules can draw wastewater because they are not completely encircled by other molecules on the surface. One of the numerous solid materials used in the adsorption technique was "activated carbon". When compared with other solid materials used in the extensively used for adsorption, Activated Carbon (AC) has the largest surface area for adsorbing both oil and in-oil substances from wastewater over a long period (Al-Hassan & Shakir, 2024). The results were successful when compared to activated carbons made from industrial waste, which remove oil pollutants using porous media (adsorbents) (Ahmed *et al*., 2024). This treatment was used because it is effective at eliminating oil pollutants from wastewater and uses very little energy because it runs at room temperature and atmospheric pressure (Ibrahim *et al*., 2023).

Extra supports of this knowledge were assumed to include the wide availability of adsorbents and the ease of regeneration of wasted adsorbents. Adsorbents that selectively adsorb oil-containing materials via chemisorption and physisorption come into direct contact with wastewater throughout the adsorptive oil development (Nawaf & Abdulmajeed, 2024). Physical adsorption, infrequently referred

to as physisorption is a reversible process that is mostly caused by weak van der Waals interactions (Mousa Al-Zobai & Hassan, 2022). On the other hand, when the attractive forces between the activated carbon and wastewater are almost as strong as covalent chemical bonds, chemisorption occurs. This is a form of monolayer adsorption in which contaminants and AC undergo a chemical reaction, where AC forms bonds with the pollutants and removes them from the water (Naser *et al*., 2021). Porous glass, zeolite, alumina, and metal-supported activated carbons were among the adsorbents that could work. Even with developments (i.e., adding functional groups and other lively sites to the adsorbent surface) and microstructural flaws, none of these adsorbents could positively eliminate oil molecules, mainly oil pollutants, from refinery wastewater (Qureshi *et al*., 2020a).

The creation of adsorbents with high adsorption capacity and discrimination for oil molecules has attracted a lot of attention (Farise *et al*., 2021). The literature that is currently available demonstrates that hardly any research has been done on the adsorptive oil by activated carbon (Qureshi *et al*., 2020b). It has been reported that treating carbon resources with alkali agents like potassium hydroxide and sodium hydroxide, professionally upsurges their surface area by causing numerous defects owing to the strong chemical etching result of the agents, mainly potassium hydroxide (KOH), and the addition of complexes comprising oxygen (Islam *et al*., 2017). The purpose of this study is to chemically treat prepared activated carbon from Plastic Waste (PW) and Upholstery Waste (UW), respectively, with activation by potassium hydroxide as an alkali agent and investigate how the treatment affects the effectiveness of oil pollutants from refinery wastewater under various operating conditions of pH, time, agitation speed, and dose. This work also inspects the isothermal models of oil adsorption in refinery wastewater.

Theoretical aspects: The relationship between the quantity of oil pollutants adsorbed and its refinery wastewater in the symmetric solution is known as the adsorption model. Depending on the adsorption model being second-hand, this test permits the entire adsorption volume of an assumed prepared activated carbon to remain as planned (Naeem & Hassan, 2018). The two different replicas which were used to find the best one between them for oil adsorbent on the surface of prepared activated carbon from UW and PW were Freundlich and Langmuir with Equations (1) and (2) correspondingly, which is valid for monolayer adsorption, where the untested isotherms were inspected. This model provides the same adsorption vitalities but with an insufficient number of locations (Jafer *et al*., 2019).

$$q_e = \frac{q_m K_L C_e}{1+K_L C_e} \quad (1)$$

where q_e is the quantity of oil adsorbed, C_e is the oil pollutants at equilibrium, K_L is the Langmuir coefficient, and q_m is the adsorption capacity.

The Freundlich Equation (6) can be practical for adsorbent multilayer adsorption.

$$q_e = K_F \, C_e^{1/n} \quad (2)$$

where K_F is the Freundlich constant connected to adsorption capacity and n is the heterogeneity limit that specifies the model (Abdul Majeed & Sabar, 2017).

Experimental Work

Material and Analytical Test

Sodium hydroxide, potassium hydroxide, hydrochloric acid, sulphuric acid, and potassium hydroxide were purchased from India and directly used without further purification. Refiner wastewater with high oil concentration was measured by UV-Vis spectrophotometer. At the end of the test, 40 mL of wastewater was placed in a closed cylinder to avoid disturbing the oil emulsion. Then, 4 mL of n-hexane was added under acidic conditions (pH = 2), followed by vigorous shaking for three minutes. After 15 minutes, once the solution had separated into two distinct layers, the upper (oil) layer was collected for absorbance measurement. The oil content in the Refinery Wastewater (RWW)

Table 1: Physical characteristics of RWW

Parameters	Oil Pollutants (OP) (mg/L)	pH	Turbidity (TUR) (NTU)	TSS (ppm)	Conductivity (ms/cm)
Value	415.88	6.89	104	17.9	145

was then determined using the calibration curve (Ahmed *et al*., 2021). The description of RWW is shown in Table 1.

Preparation of Activated Carbon

The activated carbon was prepared from upholstery waste and plastic waste by carbonaceous method from local Iraqis. The polymer wastes were cleaned to remove any dirt that might have adhered, dried, and chopped to a size of 0.5 mm to 1 mm. The treated polymer waste was impregnated with 0.5 M of NaOH for 24 hours to remove any impurities in the treated wastes. The pre-treated waste material was carbonised in a controlled environment (often in a furnace without oxygen) at a temperature of 600°C to remove volatile components and a porous carbon structure was formed.

The Activation of Activated Carbon

Firstly, AC was washed with distilled water and then dried at 110°C until a constant weight was attained. Chemical activation of AC was performed using alkali agents via a wet impregnation process. Activation solutions were made by dissolving a specific amount of the before-stated potassium hydroxide in distilled water (to get 1 M) and using a magnetic stirrer to agitate for an hour. 5 g of dried activated carbons were then treated for three hours at room temperature while being stirred and refluxed in the activation solutions. While subsequently filtering the mixture, the AC was cleaned with distilled water and diluted hydrochloric acid, dried at 110°C for the entire night, and stored in a desiccator over a desiccant (Shihab *et al*., 2020). The three-hour activation time was designated when they used prepared activated carbon treated with KOH to remove oil chemicals; as longer times had a detrimental result on the removal effectiveness of oil pollutants.

Oil Removal Experiments

The efficiency of organic removal in wastewater was evaluated in batch adsorption by prepared activated carbon. The work inspected the impact of four operational parameters on the elimination efficiency of oil pollutants: pH, agitation speed, dose, and contact duration. Each experimental trial handled 150 mL of oil pollutants as shown in Figure 1. Other parameters were kept constant because they were not inspected in this work. Following a specified adsorption period, the mixture was filtered to eliminate the adsorbents, and a spectrophotometer was used to determine the filtrate's overall oil content. A UV-Vis spectrophotometer (Shimadzu UV-1800, Japan) was used to determine the variation in the oil concentration in RWW during the adsorption treatment. Equations (3) and (4) were used to determine the oil elimination efficiency (Y%) and adsorption capacity (qt) of AC and KOH/AC, correspondingly.

$$Y\% = \left[\frac{C_o - C_t}{C_o}\right] * 100\% \quad (3)$$

$$q_t = V\left[\frac{C_o - C_t}{w}\right] \quad (4)$$

where:

C_o and C_t are the initial and any time oil content (ppm), correspondingly; V is the RWW volume and w is the activated carbon (gm).

Experimental Design

In this study, the optimal conditions for RWW treatment using batch adsorption were determined using the Box–Behnken Design (BBD) method. The independent variables of contact time are (X_1), pH (X_2), rpm (X_3), and dose (X_4). They were coded finished low and high levels in the BBD that is shown in Table 2.

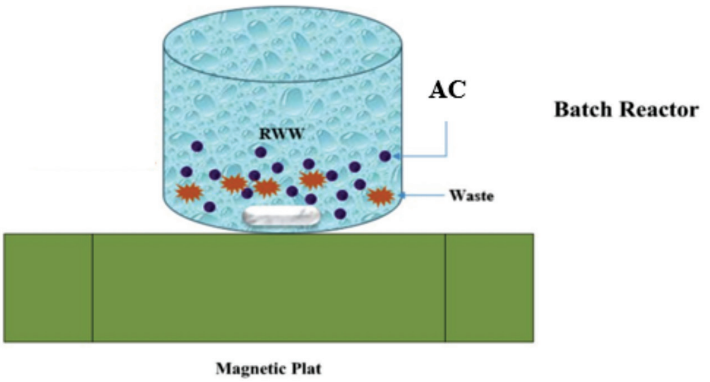

Figure 1: Batch adsorption for RWW by activated carbon

Table 2: Employed limits

Limits	Ranges
X_1: Adsorption time (min)	30-120
X_2: pH	3-9
X_3: rpm	100-300
X_4: Dose (gm)	0.2-1

Results and Discussions

Examination of the Activated Carbon Morphology

Fourier Transform Infrared (FTIR) spectroscopy demonstrates that the adsorption treatment meaningfully affects the structure of AC1 and AC2 in Figures 2 (a) and (b), correspondingly. The region from 3,000 cm^{-1} to 3,550 cm^{-1} in the FTIR spectroscopy analysis corresponds to –OH stretching vibrations, which were mostly associated with the amount of hydroxyl groups in AC samples (Nawaf & Hassan, 2025). The relative intensities in this range drop subsequent treatment of oxidation, signifying a notable decrease for current group. The mechanical qualities of treated activated carbon were lost because of this decrease in the partial breakage of hydrogen bond structures in prepared activated carbon. FTIR analyses of the AC with KOH were carried out to characterise functional groups on their surfaces and follow any potential structural change because of the treatment with an alkali agent (Nawaf *et al*., 2025).

In the X-ray Diffraction (XRD) analysis presented in Figure 3, the characteristic peaks of the prepared activated carbon sample specify a sodality structure, consistent with standard peaks of activated carbon. The distinctive peaks of the carbon structure were signified through two broad characteristic diffraction peaks that emerge in two varieties (about 20° to 30° and 40° to 50°) (Kemarau *et al*., 2024). The particles display an unchanging, polyhedral, almost hexagonal or spherical particle line structure.

The grains were arranged in sizes ranging by 500 µm sieve analysis with Field Emission Scanning Electron Microscopy (FESEM) picture in Figure 4 for AC2 and AC1 samples, respectively. The surface of the prepared KOH/AC indicates the distribution of OH^- groups over the activated carbon support. An excellent distribution of hydroxide ions was observed across the support surface. The characteristic different pores of prepared samples of activated carbon were marked in the triangular, and the FESEM picture showed randomly distributed grains with smaller sizes. From the FESEM test, it can be concluded that the formation of microparticles has a homogeneous shape structure and it was grown in very high density with almost uni-form spherical shapes. Table 3 shows the properties of AC prepared from UW and PW, correspondingly.

Energy Dispersive X-ray (EDX) determination was conducted to assess the purity of AC from PW and UW obtainable in Figures 5 (a) and (b), respectively. The analysis revealed the presence of Ca, P, C, and O elements in

the prepared samples, as listed in Table 3. No impurity peaks were observed, indicating high sample purity and confirming the presence of the intended elements. Optical analysis was used to determine the characteristics of the prepared activated carbon derived from UW and PW, respectively (Alfattal & Abbas, 2019).

The thermogravimetric curves of the prepared activated carbon produced by carbonisation and activation through alkali agents from PW and UW are shown in Figures 6 (a) and (b), respectively. The main cause of the early weight loss noticed up to 105°C was the evaporation of water from the prepared samples. The formation of upholstery waste through carbonisation and potassium hydroxide conduct enhances the thermal stability of AC, perhaps because of partial destruction of the crystalline area. This is a change in the molecular structure, by way of observation in the Thermogravimetric Analysis (TGA) curves, which was related to thermal decomposition (Mhawesh & Abd Ali, 2020). Furthermore, the thermal transitions in this temperature range were associated with the onset of thermal degradation of activated carbon, including the rearrangement of molecular chains. Using a Brunauer–Emmett–Teller (BET) test, the prepared activated carbon sample's surface area and pore volume were examined. It was found that the surface area derived from the current investigation is 154.1 and 130 m^2/g for AC2 and AC1, respectively, suggesting that there may have been changes in sample preparation, untried setup, or logical approaches between works (Pandi *et al*., 2021), as shown in Figures 7 (a) and (b), for AC1 and AC2, respectively.

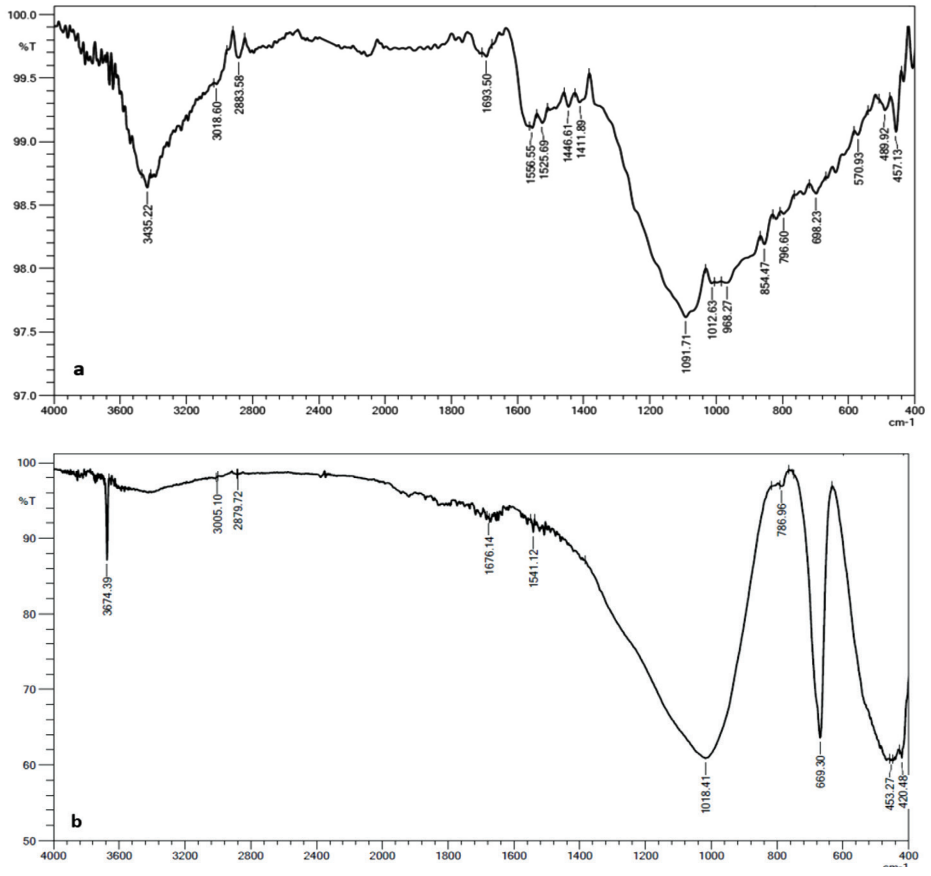

Figure 2: FTIR test of (a) AC1 and (b) AC2 samples

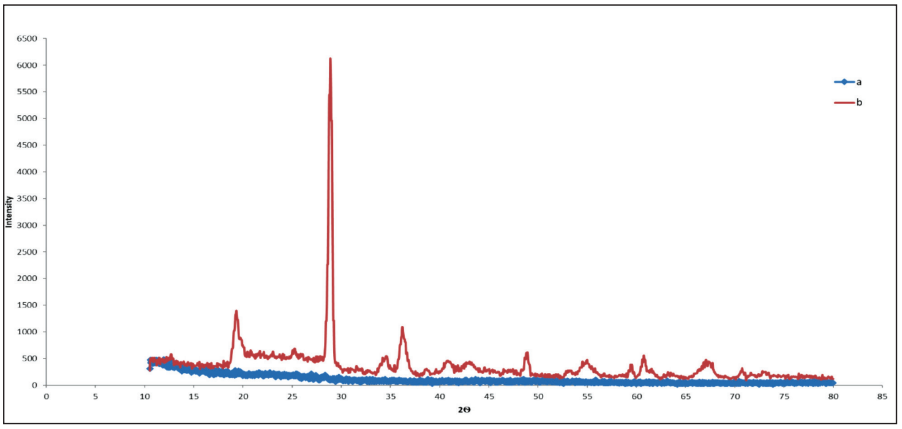

Figure 3: XRD patterns of (a) AC2 and (b) AC1

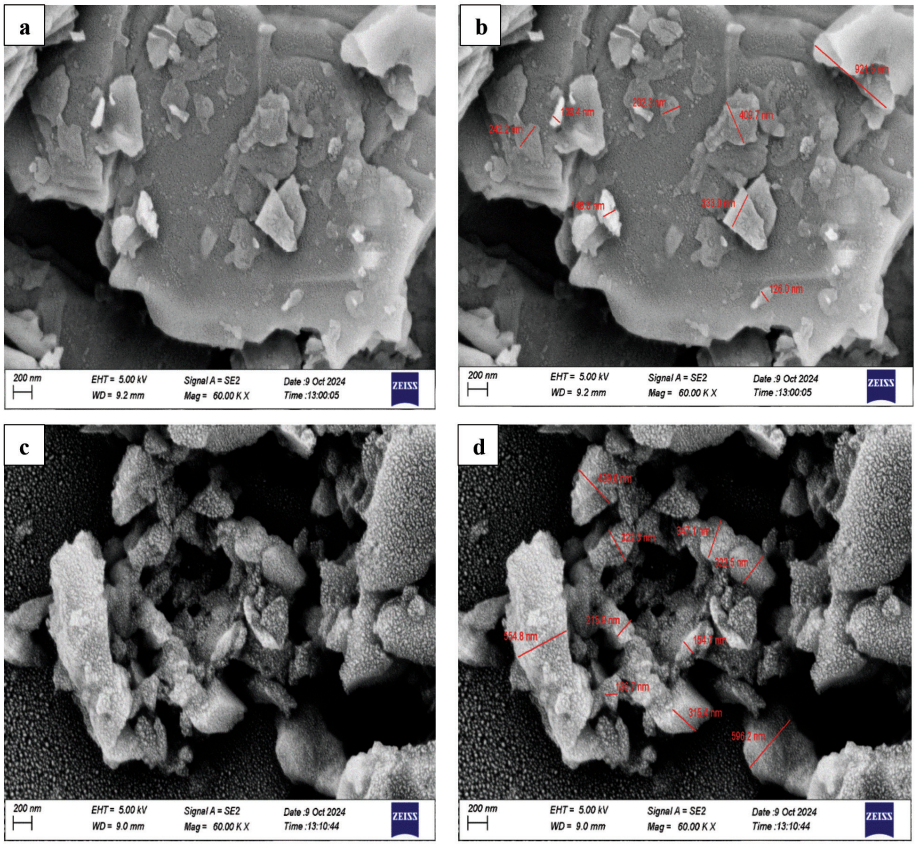

Figure 4: FESEM test of (a-b) AC2 and (c-d) AC1 at 200 nm

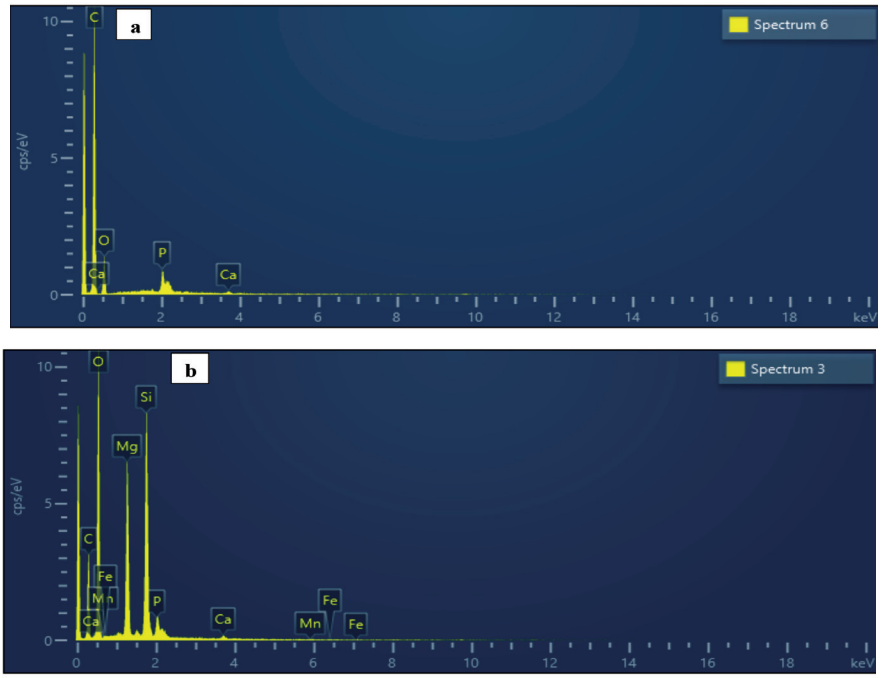

Figure 5: EDX test of (a) AC1 and (b) AC2

Table 3: EDX of prepared activated carbon

Element	AC1		AC2	
	Wt%	Atomic%	Wt%	Atomic%
C	75.52	81.33	29.98	39.29
P	2.32	0.14	1.23	0.63
Ca	0.43	0.14	0.32	0.13
O	21.73	17.56	49.25	48.47
Total	**100.00**	**100.00**	**100.00**	**100.00**

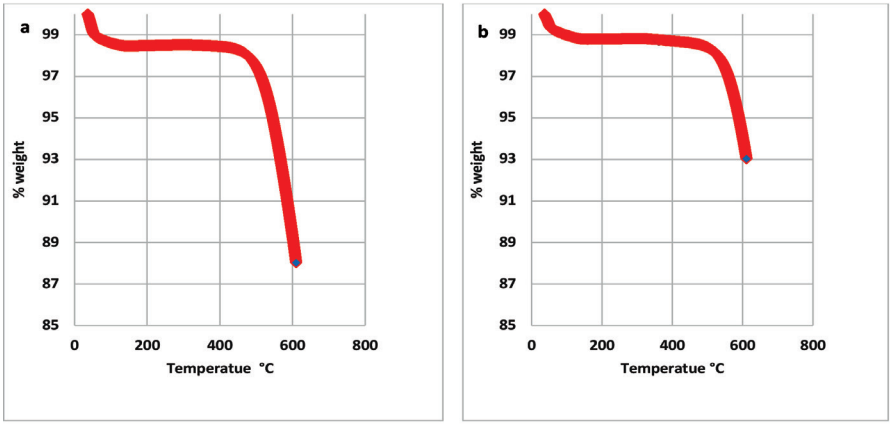

Figure 6: TGA curves of (a) AC1 and (b) AC2

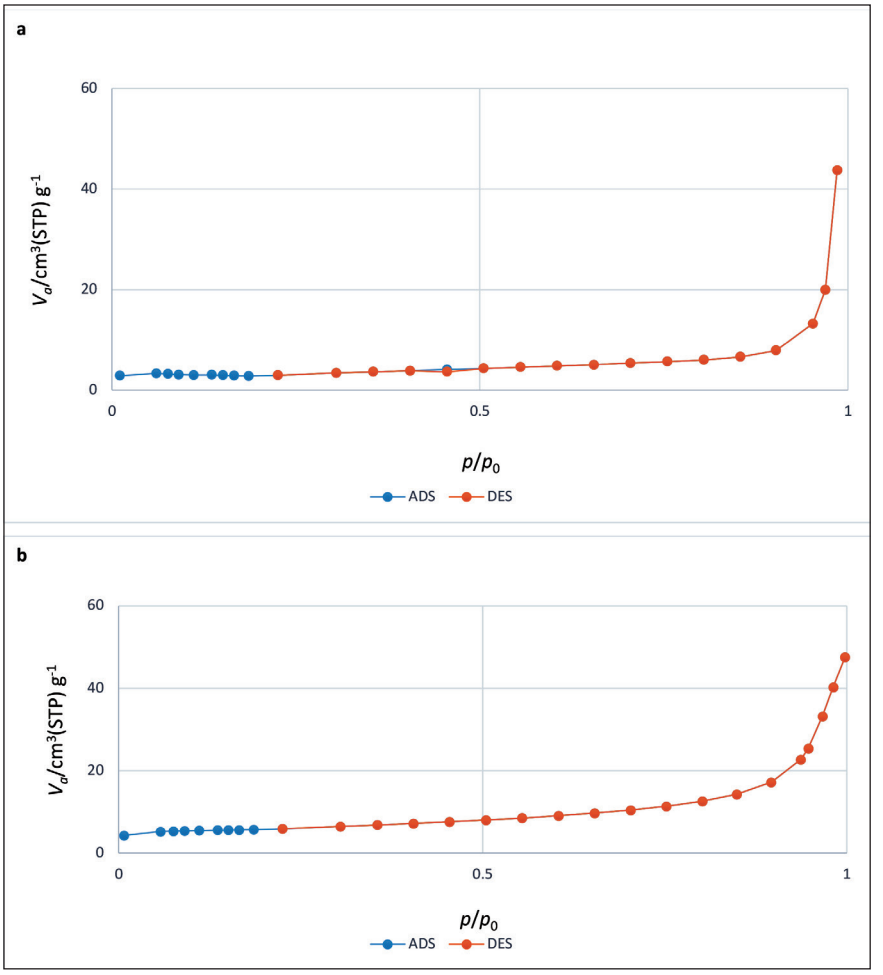

Figure 7: Isotherms of adsorption–desorption of (a) AC1 and (b) AC2

Regression Model

The final oil pollutants in RWW (27 tests were conducted by BBD) and the elimination competence response at each AC1 and AC2 on the oil adsorption treatment run were explained in Table 4. The mathematical equation [Equations (5) and (6)] were manufactured in terms of actual factors connecting the oil elimination response to the active variables, representative of the interconnections between these variables, and was found on investigative consequences.

$$\text{Oil removal by AC1} = 41.6 + 0.227\,X_1 - 1.18\,X_2 + 0.011X_3 + 62.9\,X_4 - 0.00071\,X_1^2 + 0.049\,X_2^2 + 0.000227\,X_3^2 - 15.0\,X_4^2 + 0.0013\,X_1X_2 - 0.00089\,X_1X_3 - 0.003\,X_1X_4 - 0.0005\,X_2X_3 - 1.23\,X_2X_4 - 0.0787\,X_3X_4 \quad (5)$$

$$\text{Oil removal by AC2} = 39.6 + 0.244\,X_1 - 0.94\,X_2 + 0.043X_3 + 68.4\,X_4 - 0.00058\,X_1^2 + 0.073\,X_2^2 + 0.000175\,X_3^2 - 19.3\,X_4^2 - 0.0031\,X_1X_2 - 0.000133\,X_1X_3 - 0.014\,X_1X_4 - 0.0021\,X_2X_3 - 0.075\,X_2X_4 - 0.087\,X_3X_4 \quad (6)$$

Table 4: Results of the BBD experiments

No.	Time (min) X_1	pH X_2	Agitation Speed (rpm) X_3	Dose (ppm) X_4	Oil Removal by AC1 (%)	Oil Removal by AC2 (%)
1	30	3	200	0.6	71.3	75.4
2	120	3	200	0.6	80.9	85.3
3	30	9	200	0.6	63.5	70.4
4	120	9	200	0.6	73.8	78.6
5	75	6	100	0.2	50.6	54.1
6	75	6	300	0.2	66.9	69.4
7	75	6	100	1	85.9	90.5
8	75	6	300	1	89.6	92.4
9	30	6	200	0.2	65.9	68.4
10	120	6	200	0.2	77.8	80.5
11	30	6	200	1	78.9	82.4
12	120	6	200	1	90.6	93.5
13	75	3	100	0.6	83.5	86.4
14	75	9	100	0.6	78.4	82.5
15	75	3	300	0.6	91.6	94.5
16	75	9	300	0.6	85.9	88.1
17	30	6	100	0.6	70.5	74.9
18	120	6	100	0.6	78.9	83.2
19	30	6	300	0.6	80.5	84.9
20	120	6	300	0.6	87.3	90.8
21	75	3	200	0.2	75.6	78.6
22	75	9	200	0.2	67.4	70.4
23	75	3	200	1	88.6	92.3
24	75	9	200	1	74.5	80.5
25	75	6	200	0.6	77.9	81.9
26	75	6	200	0.6	78	81.6
27	75	6	200	0.6	78.1	82.8

Analysis of Variance (ANOVA) was established in Tables 5 and 6 with a focus on the adsorption response surface model of AC1 and AC2 samples, correspondingly. The results showed the Fisher-value, *p*-test value, adjusted sum of squares (Seq. SS), adjusted mean of squares (Adj. MS), degree of freedom (DOF), and sum of squares for all limits. Just 8.89% of the total variants were not reinforced by schooling, according to the model's multiple correlations constant, which was 91.6% compatible with the statistical significance of the regression. Figure 8 shows that the adjusted manifold correlation coefficient and R^2 matched well in this model for two samples (Jafer *et al*., 2023).

The results in Figures 9 (a) and (b) explained the high competence response of elimination along the contact time of all values of the oil removal by AC2 and AC1, correspondingly. When compared between two preparations of activated carbon, the two preparations where

Table 5: ANOVA for oil removal by AC1

Foundation	DOF	Seq. SS	Adj. MS	Fisher-value	*p*-test Value
1-model	14	1774.59	126.756	2.78	0.042
Linear	4	1621.74	405.435	8.89	0.001
X_1	1	287.14	287.141	6.3	0.027
X_2	1	192	192	4.21	0.063
X_3	1	243	243	5.33	0.04
X_4	1	899.6	899.601	19.73	0.001
Square	4	103.59	25.898	0.57	0.691
X_1^2	1	11.15	11.149	0.24	0.63
X_2^2	1	1.04	1.04	0.02	0.882
X_3^2	1	27.4	27.401	0.6	0.453
X_4^2	1	30.61	30.613	0.67	0.428
2-way interaction	6	49.26	8.209	0.18	0.977
X_1*X_2	1	0.12	0.122	0	0.96
X_1*X_3	1	0.64	0.64	0.01	0.908
X_1*X_4	1	0.01	0.01	0	0.988
X_2*X_3	1	0.09	0.09	0	0.965
X_2*X_4	1	8.7	8.703	0.19	0.67
X_3*X_4	1	39.69	39.69	0.87	0.369
Error	12	547.04	45.587		
Lack-of-fit	10	547.02	54.702	5470.19	0
Pure error	2	0.02	0.01		
Total	**26**	**2321.63**			

high elimination at an acid solution had a strong interaction directed to Oil Pollutant (OP) and vice versa to pH on the oil elimination, where increasing the pH led to reduction the oil elimination. This is because there is an interaction between the OP in RWW and the prepared AC due to the van der Waals forces and high surface area of the adsorbent. Figures 9 (a) and (b) show the adsorption time, rpm concentration, and dose, respectively, ranging from low to high (El Kaim Billah *et al*., 2023).

The data were examined using the "Minitab 17" software, and the main assumptions regarding the issues were dependable. The change in response resulting from a change in the level of an issue still determines its consequence. This was commonly referred to as the major effect because it tackles the primary issues of interest in the testing (Alamery & Hassan, 2022). Figures 10 (a) and (b) validate the key components of each restriction on the OP of AC2 and AC1 adsorption, correspondingly. The dose, pH, and time have the biggest effects on the elimination of oil in RWW. In the range under work, this constant, which has a positive sign, indicates how rising rpm and dose as well as time would upsurge oil elimination, and on the other hand, how cumulative pH would reduce oil elimination (Kurniawan *et al*., 2023).

The best settings for enhanced working variables including pH, rpm, dose, and contact time were still established. Figure 11 shows the measurement effects of the D-optimisation for the adsorption of OP in refinery wastewater (Hassan & Shakir, 2024).

Table 6: ANOVA for oil removal by AC2

Foundation	DOF	Seq. SS	Adj. MS	Fisher-value	*p*-test Value
1-model	14	1774.61	126.76	3.34	0.021
Linear	4	1611.71	402.93	10.63	0.001
X_1	1	256.69	256.69	6.77	0.023
X_2	1	147	147	3.88	0.072
X_3	1	196.02	196.02	5.17	0.042
X_4	1	1012	1012	26.7	0
Square	4	110.8	27.7	0.73	0.588
X_1^2	1	7.42	7.42	0.2	0.666
X_2^2	1	2.31	2.31	0.06	0.809
X_3^2	1	16.26	16.26	0.43	0.525
X_4^2	1	50.98	50.98	1.34	0.269
2-way interaction	6	52.1	8.68	0.23	0.959
X_1*X_2	1	0.72	0.72	0.02	0.892
X_1*X_3	1	1.44	1.44	0.04	0.849
X_1*X_4	1	0.25	0.25	0.01	0.937
X_2*X_3	1	1.56	1.56	0.04	0.843
X_2*X_4	1	3.24	3.24	0.09	0.775
X_3*X_4	1	44.89	44.89	1.18	0.298
Error	12	454.82	37.9		
Lack-of-fit	10	454.04	45.4	116.42	0.009
Pure error	2	0.78	0.39		
Total	**26**	**2229.44**			

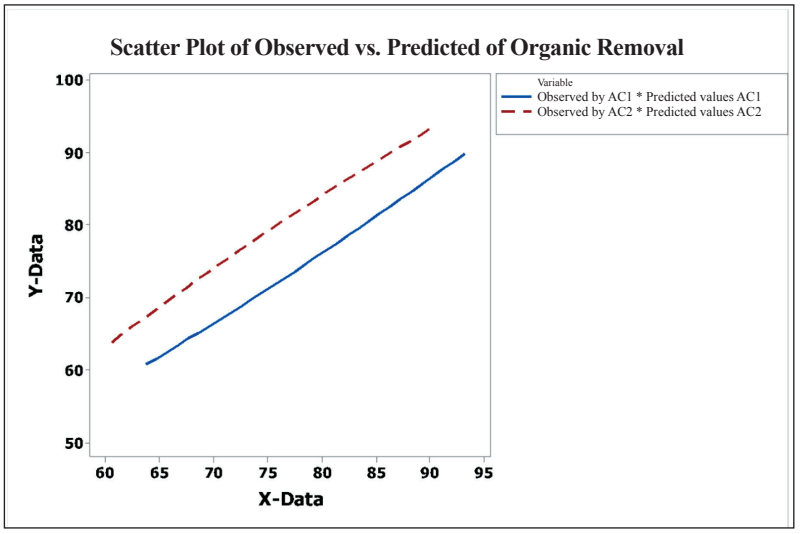

Figure 8: Observed vs. predicted values of oil removal

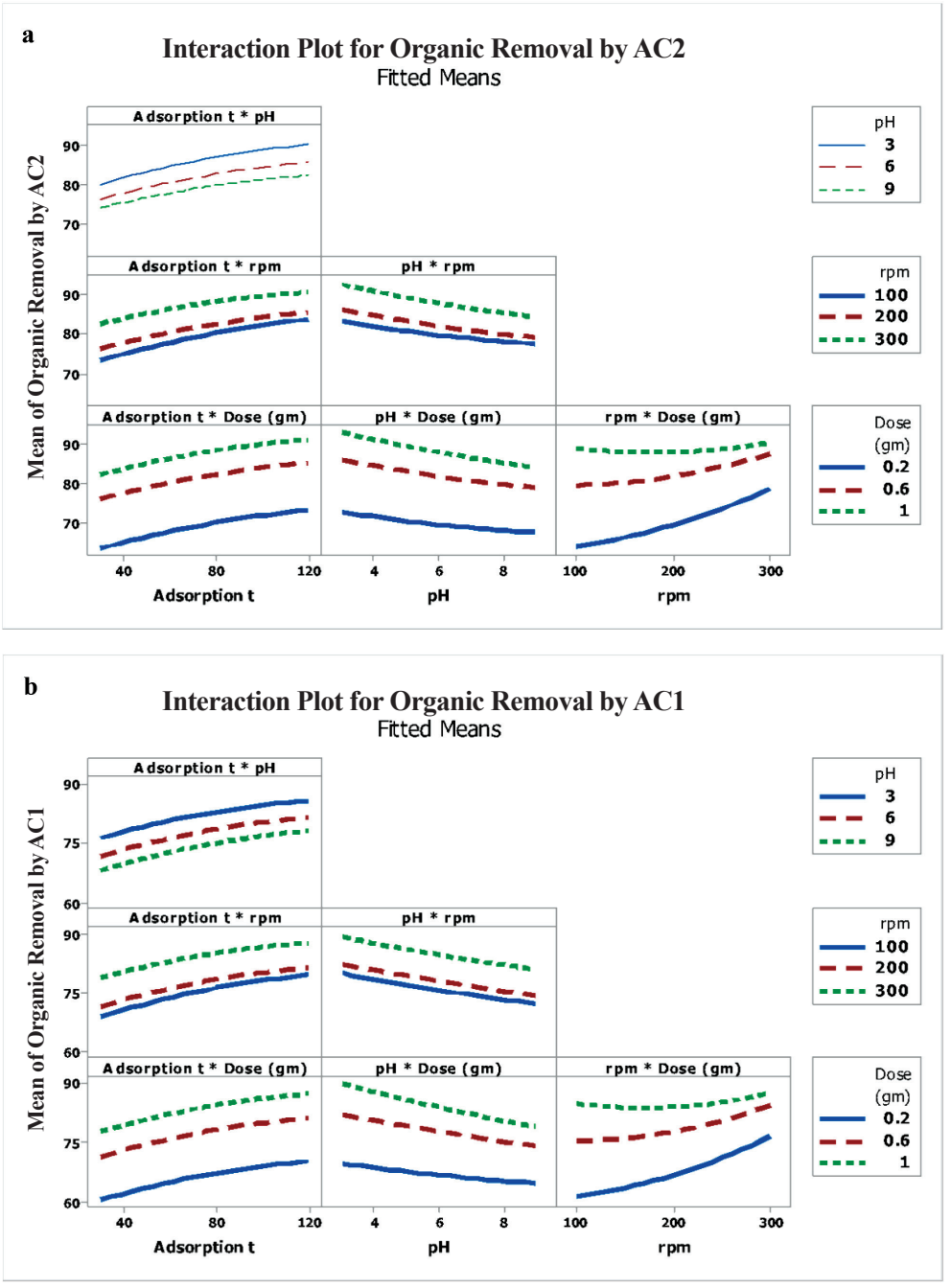

Figure 9: Interaction plot of variables of (a) AC2 and (b) AC1

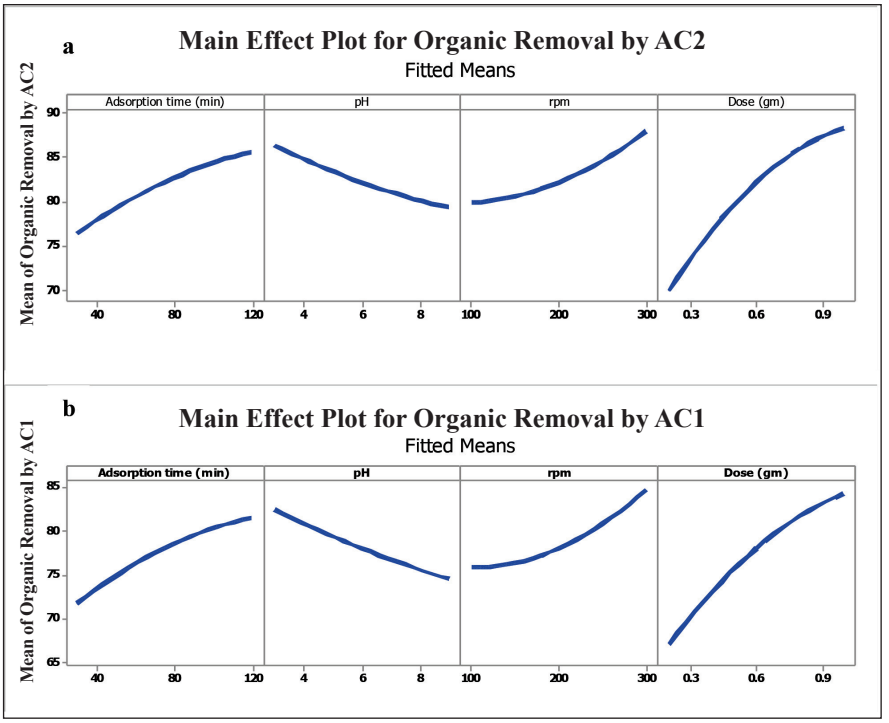

Figure 10: Impact of oil removal of (a) AC2 and (b) AC1

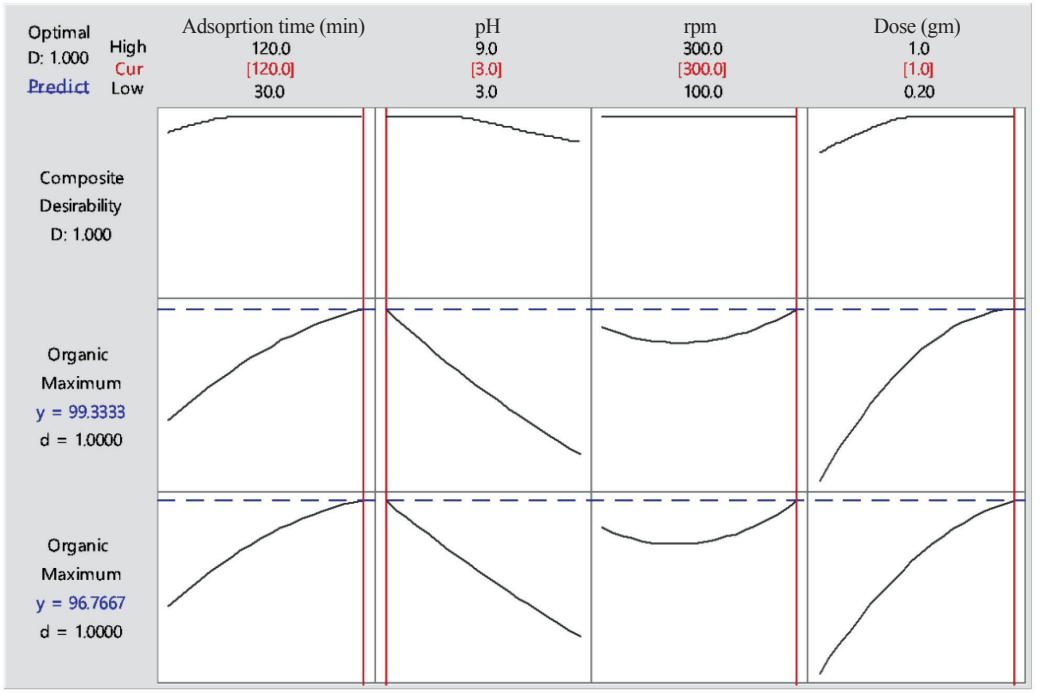

Figure 11: The best values of the working variables

Effect of Dose

The effect of dose on the ratio of OP detached from RWW with an increase in the dose leads to an increase in the oil elimination as presented in Figure 12. To upsurge the dose from 0.2 gm to 1 gm, the percentage elimination augmented from 68.1% and 71.5% to 83.1% and 87.9% at constant the other variables of AC1 and AC2, correspondingly. An increase in the dose leads to an increase in the oil removal in refinery wastewater, while the increasing adsorption locations and empty site consumption had a minor consequence on the relative oil elimination at high adsorbent amounts (Hassan & Al-Zobai, 2019).

Effect of Adsorption Time

The adsorption method was progressively augmented by the contact time. This continued for 1.5 hours, after which it remained constant. As a consequence, the equilibration duration was prudently set at 2 hours, which was carefully sufficient to ensure that this absorbent would eliminate any OP in RWW. To reserve adsorption symmetry, the adsorption duration was kept constant at 2 hours in the following tests. Prominently, the contact time arcs in Figure 13 remain flat and continuous, indicating the possibility of monolayer attention of oil contaminants on the prepared activated carbon surface from polymer waste. This occurs because the available active sites become saturated and equilibrium is reached after 2 hours (Saleh Jafer & Hassan, 2019).

Effect of Solution pH

One of the most important factors manipulating the adsorption process in RWW was pH. The rating of ionisation of the wastewater during this method and the prepared activated carbon shallow charge were both impacted via pH. H^+ can be powerfully contested temporarily through the OP intended for this treatment site. Hence, the effect of solution pH on oil pollutants adsorption in RWW was verified (Che Su *et al*., 2023). The experiments were conducted at initial pH values ranging from 3 to 9 to determine the optimal pH and prevent the precipitation of OP. The oil removal efficiencies of AC2 and AC1 were 89.1% and 82.5% at pH 3, and 81.2% and 74.3% at pH 9, respectively, as shown in Figure 14. Similar findings have been reported for the adsorption of oil contaminants (Mendra *et al*., 2024).

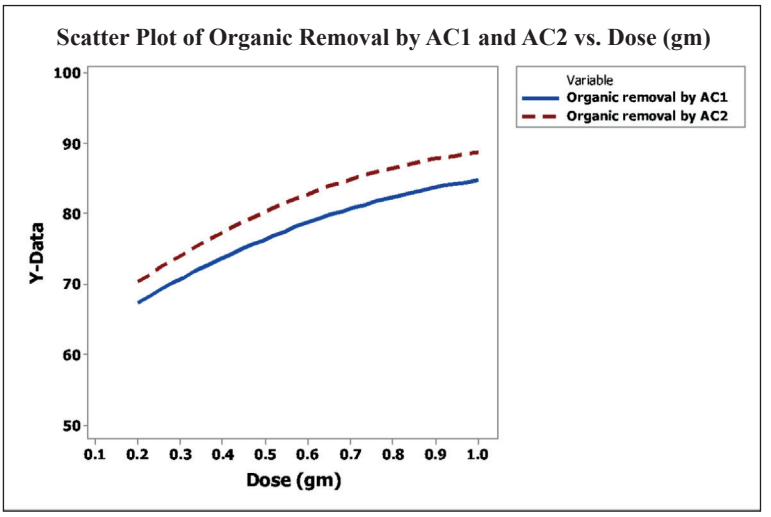

Figure 12: Effect of dose on oil elimination

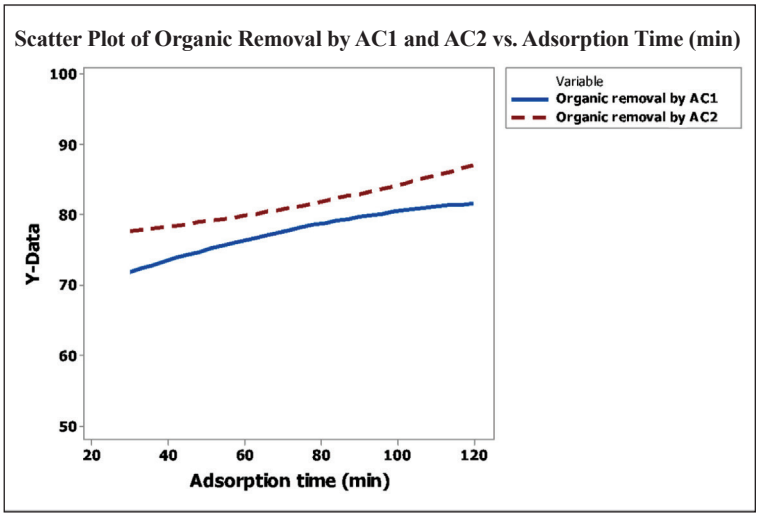

Figure 13: Effect of adsorption time on oil elimination

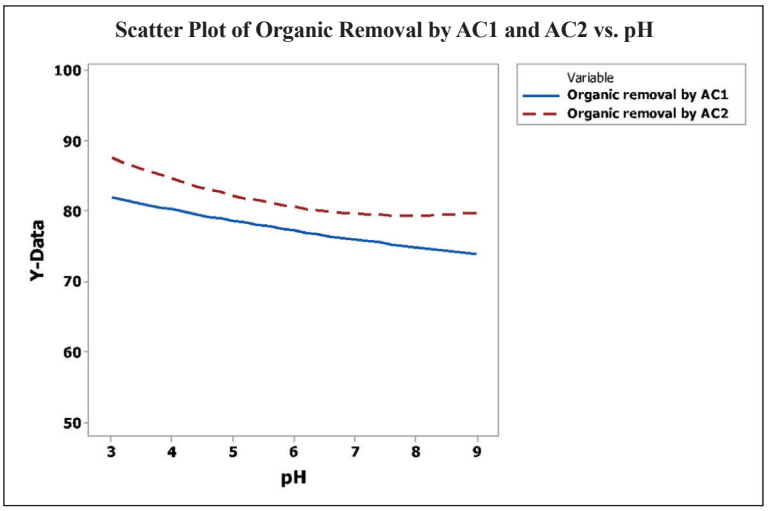

Figure 14: Effect of pH on oil elimination

Effect of Agitation

To study the effect of agitation speed on the presentation of the adsorption technique of prepared activated carbon, experimentations were tested at agitation of 100 rpm, 200 rpm, and 300 rpm. The oil removal augmented with the cumulative speed, which reached 75.1% and 79.1% to 85.4% and 81.3% at 100 rpm and 300 rpm of AC1 and AC2, correspondingly, as presented in Figure 15. A higher speed would lead to a higher mix of prepared activated carbon with oil contaminants in RWW, leading to a greater degradation of oil pollutants (Sulyman *et al*., 2021).

Freundlich, Langmuir, and isotherm equations were fitted to the adsorption data for prepared activated carbon. The dose of activated carbon was found to have a Langmuir supreme adsorption capacity of 24.3 mg/g and 21.4 mg/g of activated carbon from UW and PW, respectively. According to association

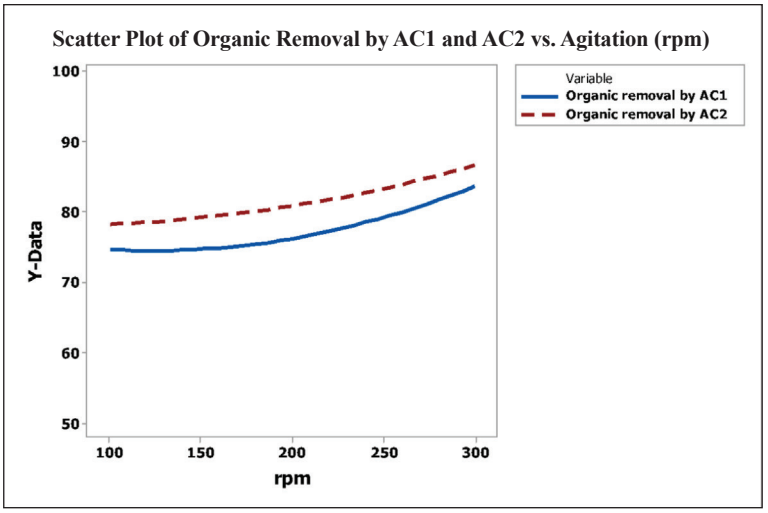

Figure 15: Effect of agitation on oil elimination

coefficients, the Langmuir model outstripped the other model in terms of how well it accounted for the evidence ($R^2 > 0.96$ and for the Langmuir model in Figures 16 (a) and (b) vs. 0.91 and for the Freundlich model in Figures 17 (a) and (b) of activated carbon from UW and PW correspondingly. In addition, this outcome is similar to the study conducted by Yin *et al*. (2023).

Mechanism of Magnetic Adsorbent for OP

The adsorption method produces a coating of oil ions, or adsorbate, on the surface of adsorbents. A desorption method (reverse adsorption, in which adsorbate ions are transported from the adsorbent surface) can be used to mimic adsorption for a range of applications because it is a reversible treatment in certain situations. The three primary processes involved in adsorption onto prepared activated carbon were the transport of the contaminant from refinery wastewater to the adsorbent surface, adsorption onto the solid surface, and transport within the adsorbent particle (Hammadi & Shakir, 2019). Adsorption of charged contaminants on differently charged adsorbents usually occurs by electrostatic attraction because oil pollutants have a great affinity for the surfaces of hydroxyl (OH^-) or other functional groups. Furthermore, attractive

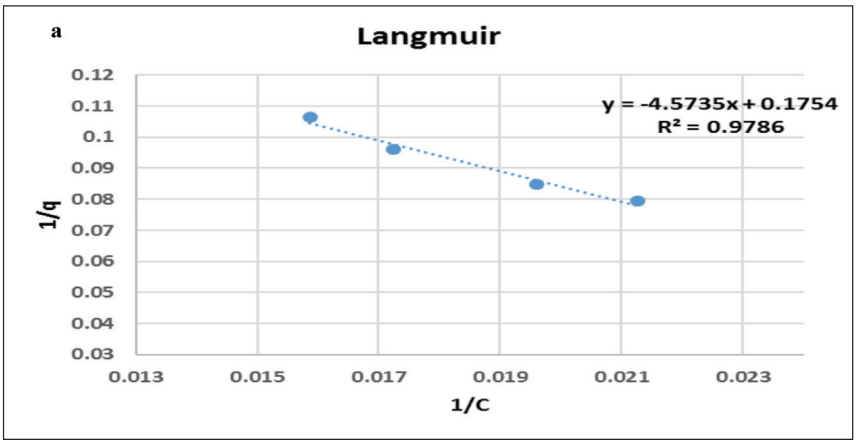

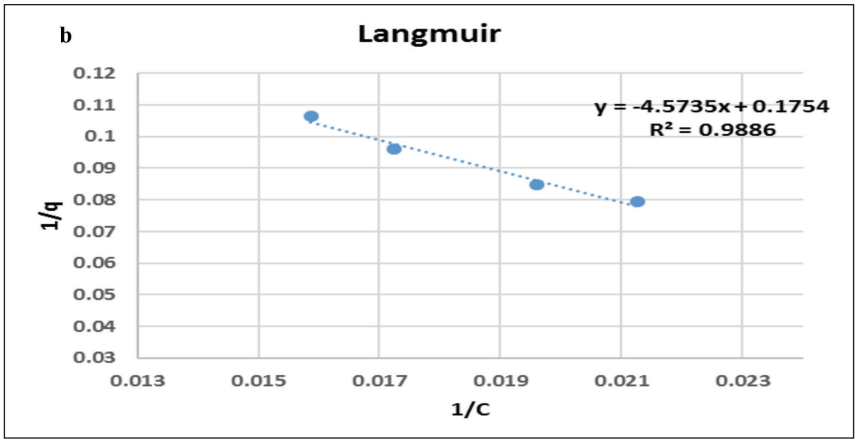

Figure 16: Langmuir model of (a) AC1 and (b)AC2

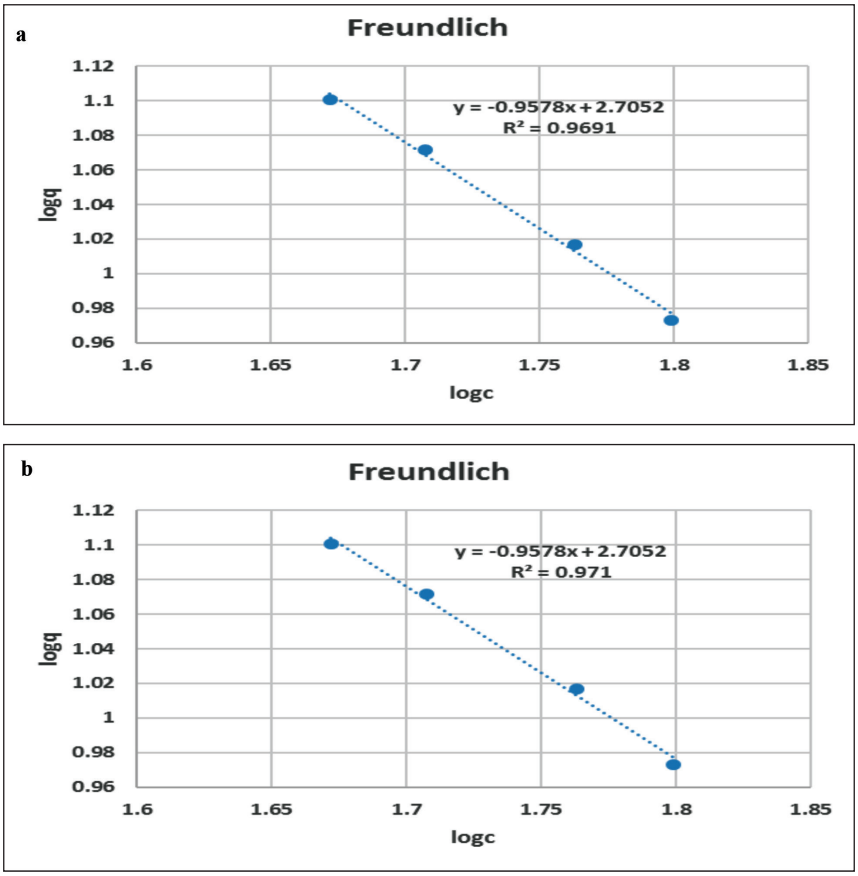

Figure 17: Freundlich model of (a) AC1 and (b) AC2

forces including hydrogen bonds, van der Waal forces, and hydrophobic interactions may be involved in the metal adsorption treatment on the surface of biosorbents as presented in Figure 18. Complexation and chelation are two more known adsorption procedures. Complexation is typically a process that occurs when numerous species come together, while chelation is one specific example that results in the development of rings (Jjagwe *et al*., 2021).

Conclusions

The consequences showed that activated carbon prepared from UW and PW by the carbonaceous method and activation by potassium hydroxide are low-cost absorbents that can be used to remove oil pollutants from refinery wastewater. The oil pollutants in RWW were eliminated using these adsorbents from activated carbon. High oil elimination efficiency of 94.7% and 90.8% of AC2 and AC1, correspondingly, demonstrated a higher adsorption efficiency. As for the enhanced electron density on the AC surface brought on by the attached hydroxyl functional groups, this was most likely caused by the development of a microporous structure of prepared activated carbon, where the Langmuir isotherm model was shadowed through the adsorption treatment.

Acknowledgements

The author would like to sincerely thank the Editorial Board and reviewers of the journal for reviewing and providing comments on the article's content.

Conflict of Interest Statement

The author declares that there is no conflict of interest.

References

Abdul-Majeed, B. A., & Sabar, D. A. (2017). Preparations of organoclay using cationic surfactant and characterisation of PVC/(bentonite and organoclay) composite prepared via melt blending method. *Iraqi Journal of Chemical and Petroleum Engineering*, *18*(1), 17-36. https://doi.org/10.31699/ijcpe.2017.1.2

Ahmed, I. H., Hassan, A. A., & Sultan, H. K. (2021). Study of electro-fenton oxidation for the removal of oil content in refinery wastewater. *IOP Conference Series: Materials Science and Engineering*, *1090*(1), 012005. https://doi.org/10.1088/1757-899x/1090/1/012005

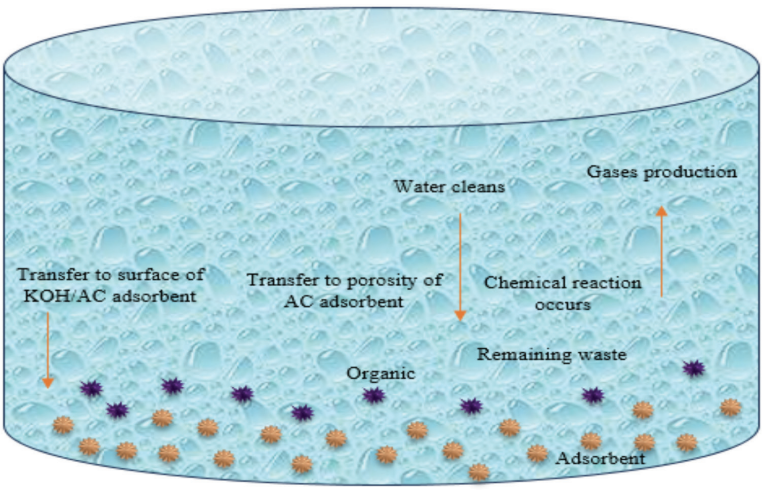

Figure 18: The mechanism proposed for the removal of oil by activated carbon

Ahmed, M. J., Anastopoulos, I., Kalderis, D., Haris, M., & Usman, M. (2024). Insight into the wheat residues-derived adsorbents for the remediation of organic and inorganic aquatic contaminants: A review. *Environmental Research*, 118507.

Al-Hassan, A. A., & Shakir, I. (2024). Enhanced photocatalytic activity of CuO/NCW via adsorption optimisation for refinery wastewater. *Iranian Journal of Chemistry and Chemical Engineering*, *44*(1), 147, 172-185.

Alamery, H. R. D., & Hassan, A. A. (2022). Effect of intensity of light and distance for decolonisation in direct red wastewater by photo fenton oxidation. *ARPN Journal of Engineering and Applied Sciences*, *17*(1819-6608), 9.

Alfattal, A. H., & Abbas, A. S. (2019). Synthesised 2nd generation zeolite as an acid-catalyst for esterification reaction. *Iraqi Journal of Chemical and Petroleum Engineering*, *20*(3), 67-73. https://doi.org/10.31699/ijcpe.2019.3.9

Che Su, N., Basirun, A. A., Hameed Sultan, N. S., Kanakaraju, D., & Wilfred, C. D. (2023). Modified nanocellulose-based adsorbent from sago waste for diclofenac removal. *Sustainability*, *15*(7), 5650. https://doi.org/10.3390/su15075650

El Kaim Billah, R., Ayouch, I., Abdellaoui, Y., Kassab, Z., Khan, M. A., Agunaou, M., Soufiane, A., Otero, M., & Jeon, B. H. (2023). A novel chitosan/nano-hydroxyapatite composite for the adsorptive removal of Cd(II) from aqueous solution. *Polymers*, *15*(6). https://doi.org/10.3390/polym15061524

Farise, S. B., Alabdly, H. A., & Hasan, A. A. (2021). Lead removal from simulated wastewater using magnetite as adsorbent with Box-Behnken design. *IOP Conference Series: Earth and Environmental Science*, *790*(1). https://doi.org/10.1088/1755-1315/790/1/012020

Hammadi, A. N., & K. Shakir, I. (2019). Adsorption behavior of light naphtha components on zeolite (5a) and activated carbon. *Iraqi Journal of Chemical and Petroleum Engineering*, *20*(4), 27-33. https://doi.org/10.31699/ijcpe.2019.4.5

Hassan, A. A. (2025). Fabrication of solar-driven new composite heterostructure $CoWO_4$/NCW photo catalysts for enhanced adsorption/photo degradation activity of organic pollutants. *Progress in Color Colorants Coating*, *18*, 201-218.

Hassan, A. A., & Al-Zobai, K. M. M. (2019). Chemical oxidation for oil separation from oilfield-produced water under UV irradiation using titanium dioxide as a nano-photocatalyst by batch and continuous techniques. *International Journal of Chemical Engineering*, *2019*. https://doi.org/10.1155/2019/9810728

Hassan, A. A., & Shakir, I. K. (2024). Synthesis of nanocellulose using ultrasound-assisted acid hydrolysis for adsorption/oxidation of organic pollutants in wastewater under UV and Solar Light. *Journal of Sustainability Science and Management*, *19*(12), 120-140. https://doi.org/10.46754/jssm.2024.12.008

Ibrahim, H. A., Hassan, A. A., Ali, A. H., & Kareem, H. M. (2023). Organic removal from refinery wastewater by using electrocatalytic oxidation. *AIP Conference Proceedings*, *2806*(1).

Islam, M. A., Ahmed, M. J., Khanday, W. A., Asif, M., & Hameed, B. H. (2017). Mesoporous activated carbon prepared from NaOH activation of rattan (*Lacosperma secundiflorum*) hydrochar for methylene blue removal. *Ecotoxicology and Environmental Safety*, *138*, 279-285. https://doi.org/10.1016/j.ecoenv.2017.01.010

Jafer, A. S., Al-Khateeb, R., Alobaid, B., Atiyah, A., & Hassan, A. A. (2023). Copper removal from produced water by photo Fenton oxidation. *AIP Conference Proceedings*, *2806*(1).

Jafer, A. S., Hassan, A. A., & Naeem, Z. T. (2019). A study on the potential of moringa seeds in adsorption of organic content from water collected from oilfield refinery. *Pakistan Journal of Biotechnology*, *16*(1), 27-33. https://doi.org/10.34016/pjbt.2019.16.1.5

Jjagwe, J., Wilberforce, P., Menya, E., & Mpagi, H. (2021). Synthesis and application of Granular activated carbon from biomass waste materials for water treatment: A review. *Journal of Bioresources and Bioproducts*, *6*(4), 292-322. https://doi.org/10.1016/j.jobab.2021.03.003

Kemarau, R. A., Eboy, O. V., & Sakawi, Z. (2024). The effect of land use change on water turbidity using remote sensing and GIS technique. *Journal of Sustainability Science and Management*, *19*(8), 1-15.

Kurniawan, T. W., Sulistyarti, H., Rumhayati, B., & Sabarudin, A. (2023). Cellulose Nanocrystals (CNCs) and Cellulose Nanofibers (CNFs) as Adsorbents of heavy metal ions. *Journal of Chemistry*. https://doi.org/10.1155/2023/5037027

Mendra, N. I., Yuria, P., Ramanta, I. W., Widanaputra, A. A. G. P., & Suaryana, I. G. N. A. (2024). The impact of corporate governance based on natural environmental sustainability, intellectual capital, and risk management on profitability and financial sustainability. *Journal of Sustainability Science and Management*, *19*(10), 8-24.

Mhawesh, T. H., & Abd Ali, Z. T. (2020). Reuse of brick waste as a cheap sorbent for the removal of nickel ions from aqueous solutions. *Iraqi Journal of Chemical and Petroleum Engineering*, *21*(2), 15-23. https://doi.org/10.31699/ijcpe.2020.2.3

Mousa Al-Zobai, K. M., & Hassan, A. A. (2022). Utilisation of iron oxide nanoparticles (hematite) as adsorbent for removal of organic pollutants in refinery wastewater. *Materials Science Forum*, *1065*, 91-100.

Naeem, H. T., & Hassan, A. A. (2018). Effectiveness & economy of sawdust wood adsorbents in removing anionic dyes of aqueous solutions. *Pakistan Journal of Biotechnology*, *15*(2), 311-320.

Naser, G. F., Dakhil, I. H., & Hasan, A. A. (2021). Organic pollutants removal from oilfield-produced water using nano magnetite as adsorbent. *Global NEST Journal*, *23*(3), 381-387. https://doi.org/10.30955/gnj.003875

Nawaf, A. T., & Abdul-Majeed, B. A. (2024). Design of oscillatory helical baffled reactor and dual functional mesoporous catalyst for oxidative desulfurisation of real diesel fuel. *Chemical Engineering Research and Design*, *209*, 193-209. https://doi.org/10.1016/j.cherd.2024.07.032

Nawaf, A. T., & Hassan, A. A. (2025). Design of (MnO_2/GO) for removal of organic compounds from wastewater using a digital baffle batch reactor. *International Journal of Environmental Science and Technology*, *22*(7), 1-20.

Nawaf, A. T., Humadi, J. I., Hassan, A. A., Habila, M. A., & Haldhar, R. (2025). Improving fuel quality and environment using new synthetic (Mn_3O_4/AC-nano-particles) for oxidative desulfurisation using digital baffle batch reactor. *South African Journal of Chemical Engineering*, *52*, 8-19. https://doi.org/10.1016/j.sajce.2025.01.003

Pandi, N., Sonawane, S. H., & Anand Kishore, K. (2021). Synthesis of cellulose nanocrystals (CNCs) from cotton using ultrasound-assisted acid hydrolysis. *Ultrasonics Sonochemistry*, *70*, 105353. https://doi.org/10.1016/j.ultsonch.2020.105353

Qureshi, U. A., Hameed, B. H., & Ahmed, M. J. (2020a). Adsorption of endocrine disrupting compounds and other emerging contaminants using lignocellulosic biomass-derived porous carbons: A review. *Journal of Water Process Engineering*, *38*, 101380. https://doi.org/10.1016/j.jwpe.2020.101380

Qureshi, U. A., Hameed, B. H., & Ahmed, M. J. (2020b). Adsorption of endocrine

disrupting compounds and other emerging contaminants using lignocellulosic biomass-derived porous carbons: A review. *Journal of Water Process Engineering*, *38*, 101380. https://doi.org/10.1016/j.jwpe.2020.101380

Saleh Jafer, A., & Hassan, A. A. (2019). Removal of oil content in oilfield-produced water using chemically modified kiwi peels as efficient low-cost adsorbent. *Journal of Physics: Conference Series*, *1294*(7). https://doi.org/10.1088/1742-6596/1294/7/072013

Shihab, M. A., Nawaf, A. T., Mohamedali, S. A., & Alsalmaney, M. N. (2020). Improving the porosity of activated carbon nanotubes via alkali agents for the enhancement of the adsorptive desulfurisation process. *Materials Science Forum*, *1002*, 423-434.

Sulyman, M., Kucinska-Lipka, J., Sienkiewicz, M., & Gierak, A. (2021). Development, characterisation and evaluation of composite adsorbent for the adsorption of crystal violet from aqueous solution: Isotherm, kinetics, and thermodynamic studies. *Arabian Journal of Chemistry*, *14*(5), 103115. https://doi.org/10.1016/j.arabjc.2021.103115

Yin, Z., Liu, S., Tian, Z., Zhao, X., He, J., & Wang, C. (2023). Carbon-based nanomaterials mediated adsorption and photodegradation of typical organic contaminants in aqueous fulvic acid solution. *Water Science and Technology*, *88*(7), 1863-1874. https://doi.org/10.2166/wst.2023.300